Polar Lows

(Article No. 317)

Ian A. Renfrew, British Antarctic Survey, Natural Environmental Research Council, Cambridge, UK.

Introduction

Through the years mariners of the Nordic Seas have told tales of unexpected encounters with fierce storms that appeared out of nowhere to wreak havoc on the seas. These storms were smaller and more transient than the more predictable synoptic-scale weather systems that were familiar. Yet with the advent of the satellite era, it appeared these smaller scale vortices were ubiquitous over the polar seas. The high latitude location of these storms, and their identification as low pressure centres, led to them becoming known as polar lows; although a host of alternative names have been used in reference to such weather systems, for example, Arctic instability lows, comma clouds and, in the Southern Hemisphere, Antarctic coastal vortices. Polar lows are now defined as intense maritime cyclones with scales less than 1000 km and near-surface wind speeds in excess of 15 m s^{-1}. Polar lows are the most intense example of the family of mesoscale cyclonic vortices, poleward of the main polar front, known generically as polar mesoscale cyclones. This article will discuss both, but will focus on those more energetic systems known as polar lows.

Polar lows are characterized as subsynoptic in scale, typically 100 to 500 km in diameter, and short lived, typically lasting only 3 to 36 hours. They develop over water, but often move over land or ice where they tend to fade rapidly. In terms of dynamics, polar lows are fundamentally baroclinic or convective in nature. In most cases, some element of convection is necessary for rapid development to an intense polar low. Purely baroclinic, or topographically forced, systems tend to remain as weaker polar mesoscale cyclones. One of the most prominent hallmarks of a polar low is the spiral of cloud associated with the vortical flow (**Figure 1**). Occasionally there is a clear eye at the centre of the cloud vortex suggesting an analogy with tropical cyclones, indeed such systems have been described as Arctic hurricanes. More often than not they are warm cored vortices, and many have well-defined fronts, suggesting parallels with synoptic-scale extratropical cyclones.

The distribution around the globe of the land-masses, sea ice and sea surface temperatures leads to some favored locations for the development of intense polar lows. These are regions prone to cold-air outbreaks, where relatively cold continental air is advected over relatively warm ice-free waters. For example, in the Nordic Seas (the

Greenland, Iceland, Norwegian and Barents Seas), the Labrador Sea, the Bering Sea, the Gulf of Alaska and the Sea of Japan. In the Southern Hemisphere, the eastern Weddell, the Bellingshausen and the Ross Seas are favored locations. Satellite-based climatological studies show there are typically hundreds of polar mesoscale cyclones per year in each of these regions. In the Northern Hemisphere, polar mesoscale cyclone development is most common during winter, followed by the autumn and spring seasons. In the Southern Hemisphere, there appears to be no significant seasonal variability, but there are preferences in location that tend to be dictated by variations in the sea ice distribution.

Polar lows are extremely important weather systems for certain regions as their strong winds and severe weather are potentially hazardous. However it is also likely that polar mesoscale cyclones play an important but as yet unclear role in the climate system at high latitudes; for example, through a strong coupling of the polar atmosphere and ocean through air-sea heat exchange.

Observations of polar low structure

Polar mesoscale cyclones are relatively small scale and short lived, which makes them difficult to observe by conventional means as they tend to fall between the spatial and temporal gaps in the observing network. Their location in sparsely populated or maritime regions compounds this difficulty. With the advent of the satellite era, and the development of satellite remote sensing as a tool for meteorological observation, our knowledge has vastly improved; not least in simply providing visible and infra-red images, showing the cloud structures associated with the systems (e.g. **Figures 1, 2**).

Instrumented aircraft data

The availability of satellite imagery in real time has allowed the targeting of incipient polar lows for further investigation by instrumented aircraft. Only a very small number of polar lows have been investigated by aircraft, but these few cases provide otherwise unobtainable details of their structure. One case from over the Norwegian Sea in February 1984 is discussed as an illustration. **Figure 3** shows an infra-red satellite image: light colours represent colder brightness temperatures and therefore generally higher clouds. There is a high comma-shaped cloud spiralling into the center of a mature polar low and contrasting with the warmer brightness temperatures of the sea surface beneath. To the south and east there are plumes of cloud associated with shallow convection. Further to the south is an elongated band of high cloud associated with a synoptic-scale weather system.

An instrumented aircraft made a number of passes through the polar low over a period of a few hours centered at this time. Atmospheric soundings from dropsonde releases and nearby radiosonde ascents, along with the flight-level data have been synthesized together to produce a highly detailed picture of this particular polar low. A surface pressure analysis, along with part of the aircraft track and wind observations at 300 m above sea level, is shown in **Figure 4**. Note the analysis has been time-adjusted for the motion of the low during the aircraft sampling. The low was about 400 km across with 12 mb of closed isobars. The lowest sea-level pressure recorded was 979 mb at the point of calm winds. The low was not axisymmetric, rather somewhat elongated on a northeast-southwest axis. Mesoscale fronts in these directions (dashed lines) mark a strong horizontal wind shear, where the flight-level wind barbs show abrupt changes in direction over tens of kilometres. Wind speeds were over 30 m s^{-1} in the western and southern parts of the low. The relative vorticity of the flight-level winds was an S-shape, following the mesoscale fronts, with typical values over $10x10^{-4}$ s^{-1} and peak values of twice that. The relative vorticity values were on a par with those observed in synoptic-scale extratropical cyclones. The 300-m temperature field showed a secluded warm core, 2 to 3 ^{o}C warmer than surrounding temperatures, and of a similar elongated shape to the pressure field. The low was relatively shallow with only a weak circulation signature in the mid-troposphere.

The low's vertical structure is illustrated in a cross-section of potential temperature contours and storm-relative transverse velocity vectors in **Figure 5**. The cross-section is oriented approximately north-south at about 4^{o}W. To the north (left) was a 1-km deep near-neutral marine boundary layer capped by a stable layer (bold lines). To the south (right) the marine boundary layer was about 2 km deep. In the center of the cross-section was a warm front, delineated by a strong horizontal gradient in potential temperature. There was low-level (storm-relative) convergence into the frontal region and vigorous ascent - the upward vertical velocities reaching 1 m s^{-1}. There was weaker descent on the warm side of the front, completing a cross-frontal circulation. The warm-core structure of the system is depicted by the down-welling potential temperature contours above the frontal region. Cross-sections of equivalent potential temperature showed a decrease with height up to about 2 km in the convergence region: in other words, the frontal region was unstable to moist convection. Convective precipitation was observed in this region, as radar reflectivity echoes, in a shallow layer below 3 km. Surface turbulent heat fluxes were calculated to be extremely high, up to 500 W m^{-2} for both surface sensible and latent heat fluxes. The total surface turbulent heat fluxes in this case were on a par with those observed in tropical cyclones (hurricanes). In some respects, for example the fronts and the pressure distribution, this polar low was similar to archetypal synoptic-scale extratropical cyclones (see **Extra tropical cyclones - 128**). However

the large surface turbulent heat fluxes, and clear eye (**Figure 3**) are reminiscent of tropical cyclones (see **Hurricanes - 474**).

The observations summarized above paint a vivid picture of a small-scale vortex, with remarkably strong winds, well-defined mesoscale fronts and a number of convectively unstable areas where precipitation was falling. This structure is typical of many intense baroclinic-convective types of polar low. However other case studies have shown more axisymmetric systems, with less well-defined fronts than illustrated above (e.g. **Figure 1**); or systems without areas of conditional instability, where convection is less important; or systems where upper-level forcing is vital. Clearly there is a spectrum of characteristics within the polar low category of systems. Of course this amount of structural detail is not routinely available, instead in recent years we have come to rely on satellite remote sensing for much information.

Satellite remote sensing data

The most vivid satellite observations of polar lows, and polar mesoscale cyclones, are the high resolution infra-red and visible images such as those in **Figures 1-3.** These images are simply pictures taken from space at certain wavelengths in the infra-red or visible parts of the spectrum. The highest resolution (1 km) images are from sensors on board polar orbiting satellites, for example, the Advanced Very High Resolution Radiometer (AVHRR). These provide a fantastically detailed picture of cloud structure and height, often hinting at streamlines through the shape of the clouds. Also flown on many polar orbiting satellites are vertical sounders which combine a variety of infra-red and microwave channels to obtain atmospheric emission temperatures from several heights and thus temperature or humidity profiles for an atmospheric column of order 100 km square. However the retrieval process is ill-posed, which means layer-mean temperatures, or equivalently geopotential thicknesses, are more accurate than the profiles. Nevertheless such data have been used to obtain the synoptic backdrop to polar low development and, for example, to corroborate the warm-cored nature of the polar low described above. One limitation of these sounders is their poor functionality in areas of very thick clouds, where the humidity retrievals in particular are affected. This problem is largely bypassed when a more comprehensive passive microwave sounder is used, such as the SSM/I (Special Sensor Microwave/Imager). This instrument can provide contemporaneous fields of precipitation, cloud liquid water content, and surface wind speed, at a resolution of around 100 km, although again heavy rain can interfere with the sensors. Observations from the SSM/I have helped to determine whether some mesoscale vortices are convective, or not, as convective precipitation gives a strong backscatter at certain

wavelengths. Surface wind speed can also be measured by radar altimeters (such as Geosat), again through the influence of the winds on the sea state, and thus the radar backscatter. But due to their narrow swaths these sensors only provide cross-sections through weather systems. To obtain both wind speed and wind direction from space, one has to revert to scatterometers: these are able to measure capillary waves on the ocean's surface and so infer wind speed and wind direction. They have a resolution of about 25 km, but a relatively narrow swath (typically 800 km), so at present are not able to cover the globe on a daily basis. In addition, there is an ambiguity problem in determining the wind direction. To rectify this external information, such as wind data from numerical weather prediction models, must be supplied. Surface wind data from scatterometers are at a suitable resolution for polar mesoscale cyclone investigations and have assisted in a number of case studies and climatologies. It has been shown that around 75% of cloud vortices (seen in AVHRR imagery) have a distinct surface circulation signature in scatterometer winds.

Over recent years, most operational satellite remote-sensing data have started to be incorporated, via the data assimilation processes, directly into numerical weather prediction models. This includes vertical sounder, passive microwave radiances and scatterometer data. Depending on the quality of the data assimilation and model, this should result in remotely-sensed polar mesoscale cyclones being represented in numerical weather prediction analyses and forecasts.

Dynamical theories of polar low development

A number of dynamical mechanisms have been proposed for the initiation and growth of polar lows and polar mesoscale cyclones. The two most widely-accepted theories being that polar lows are fundamentally baroclinic disturbances or fundamentally convective disturbances. A wealth of observational and numerical modeling studies would now suggest there is a continuous spectrum of polar mesoscale cyclones that spans these, and other, development mechanisms.

Baroclinic dynamics

The classic baroclinic instability mechanism, as first developed in the 1940s and 1950s, plays a primary role in the development of synoptic-scale extratropical cyclones (see **Baroclinic Instability - 76** ; **Extra tropical cyclones - 128**). Essentially a continuously stratified fluid is unstable to small amplitude perturbations if the basic state encompasses a reversal in sign of the potential vorticity gradient. The simplest archetype of baroclinic

instability is that of a zonally symmetric atmosphere, with a rigid lid of height H, a meridional potential temperature gradient Λ (equivalent to a zonal vertical shear - assuming thermal wind balance), a Coriolis force f, and a static stability N. Here the potential vorticity gradient reversal is at the boundaries. The growth rate is a linear function of $f\Lambda/N$, and the scale of the unstable waves is a linear function of NH/f. For typical mid-latitude values this yields e-folding times of about a day and fastest growing modes on the scale of several thousand kilometres. This is an order of magnitude larger than that of observed polar mesoscale cyclones; so to use this theory to explain mesoscale cyclones requires a scale reduction through a modification of the basic-state atmosphere. For a start, at high latitudes f is larger, but more importantly both H and N can be much smaller than is typical at mid-latitudes. For example, during cold-air outbreaks the atmosphere can be represented as a near-neutral marine boundary layer capped by a strongly stable free atmosphere (e.g. **Figure 5**). In this case, if the rigid lid is taken as the strongly stable capping layer this means a much reduced H, and a reduced N in the near-neutral layer, leading to fastest growing modes on about the scale of observed polar lows (**Figs. 3, 4**). A different basic state, also leading to a scale reduction, is that of a reverse shear flow; so called because the baroclinic waves propagate in the opposite direction to the thermal wind, i.e. the shallow extent of the waves means their steering level is within the reverse flow. Here weak static stabilities and strong vertical shears can combine to yield unstable modes of order 500 km.

A different paradigm of baroclinic instability is the initial value problem: where an upper-level precursor, such as an upper-level potential vorticity anomaly, induces growth at low levels. This scenario can also be envisaged through cyclonic vorticity advection and omega equation arguments, but is perhaps more transparent within an isentropic potential vorticity (PV) framework (see **Potential Vorticity - 320**). To achieve rapid growth an upper-level PV anomaly must act in synergy with a low-level baroclinic zone, i.e. a potential temperature gradient (see **Figure 6**). The induced circulation from the upper-level PV anomaly deforms the low-level temperature field into a wave, which then induces its own cyclonic circulation as potential temperature anomalies at a boundary are equivalent to PV anomalies. The upper and lower-level anomalies reinforce each other's circulation and thus mutual growth occurs. In this scenario, the scale of the disturbance is again a function of NH/f. The presence of an upper-level PV anomaly is often associated with the intrusion of the stratosphere down into the troposphere, i.e. a low dynamical tropopause. In this case, the scale height H is reduced and (as before) when this is combined with low static stabilities, growth on the scale of polar lows is induced. This type of PV-thinking has helped to explain a number of observed and modeled polar lows. It has also enabled another form of satellite remotely-sensed data to be used, as stratospheric intrusions (i.e. PV anomalies) can be detected from

their large total column ozone amounts. For example, the TOMS instrument can be used to estimate total column ozone and thus monitor upper-level PV dynamics.

Baroclinic instability mechanisms are significantly modified by the presence of moisture: latent heat is released through condensation of water vapour during ascent, and this additional heating reinforces the baroclinicity of the system and thus enhances growth. The most intense polar mesoscale cyclones tend to form as polar lows in maritime environments, where there is a ready supply of moisture, which suggests that any baroclinic dynamics are likely to be enhanced by latent heating. Indeed a number of numerical modeling case studies have found that without moist processes the modeled polar low is unable to grow to the strength observed.

Convective dynamics

The axisymmetric cloud and the presence of a clear central eye in some polar lows (e.g. **Figure 1**) has suggested that these lows may be akin to small tropical cyclones. This idea has been pursued through the modification of some tropical cyclone development theories to polar environments. One such mechanism is Conditional Instability of the Second Kind (CISK - see **Instability: Wave-CISK - 177**). This mechanism involves the organisation of cumulonimbus convection into a coherent weather system. An initial disturbance causes low-level convergence and ascent, which, in a conditionally unstable atmosphere, gives rise to latent heat release. This generates cyclonic relative vorticity that forces further low-level convergence and, by continuity, high-level divergence. The low-level convergence provides a continued source of moisture for further latent heat release and thus a positive feedback is established. The scale of CISK-driven disturbances is determined by the vertical distribution of diabatic heating during development. The growth rate is directly dependent upon the convective available potential energy (CAPE) of the atmosphere. In the polar regions during cold-air outbreaks, extremely deep conditionally unstable layers can develop, thus providing enough CAPE for polar low development. However, it has also been argued that the atmosphere does not sustain the required amounts of CAPE for long enough to allow the CISK mechanism to act as described.

An alternative convective theory is that of Wind-Induced Surface Heat Exchange (WISHE) - also know as Air-Sea Interaction Instability - see **Hurricanes - 164**. This proposes that surface sensible and latent heat fluxes are responsible for the growth of tropical cyclones and polar lows. Moist convection mixes this additional heat and moisture through the troposphere on the scale of the growing vortex. Latent heat release within the convective clouds contributes to vortex growth and as the surface turbulent heat fluxes are proportional to

the surface winds, a positive feedback is established. The theory allows an estimate of the central pressure drop within a mature system from Carnot energy-cycle arguments and known environmental conditions; for example, the observed pressure drop of the polar low in **Figure 1** is consistent with this theory.

In some sense the above two mechanisms are variations of convective closure rather than being fundamentally different. CISK relies on low-level convergence from friction, where WISHE does not, but on the other hand, it could be argued that CISK implicitly includes surface sensible and latent heat fluxes as part of the dynamics. Recent idealized numerical modeling studies have found that polar low growth is more sensitive to the parameterization of surface heat fluxes than to the parameterization of surface friction, which provides some evidence for the WISHE mechanism, but in the real world the two mechanisms are more difficult to distinguish. A common requirement for the convective theories is an initial disturbance of the basic state about which the convection can become organised. This begs the question what causes the initial disturbance? In many observational and numerical studies, it would appear that some sort of baroclinic forcing causes the initial disturbance. As described in the previous section, this may be a linear instability of a baroclinic atmosphere or an upper-level precursor inducing flow at low levels. The initial polar low can then evolve into a convectively-driven phenomenon if the conditions are right. In other cases perhaps a topographic forcing, or a barotropic forcing, cause the initial disturbance. What is clear, is that moist convection plays a central role in the development of many polar lows in a way that it does not in other extratropical cyclones.

Numerical modeling and forecasting of polar lows

In a research context, numerous case studies have shown that state-of-the-art numerical models are able to simulate polar lows, and polar mesoscale cyclones, of all varieties. In fact, numerical modeling studies have been instrumental in elucidating the different roles of the dynamical mechanisms discussed above. To capture the growth and mesoscale structure to a reasonable accuracy typically requires the parameterization of microphysical processes (including latent heat release, cloud microphysics and multi-phase precipitation); radiative and turbulent heat fluxes (including surface turbulent heat fluxes); and moist convection. If any of these physical processes is switched off, the simulated polar lows tend to be weak or non-existent. It is also essential that the numerical model's grid resolution is suitable for the scale of the cyclone. Typically horizontal grid squares of 20-50 km are required for a cyclone of a few hundred km and higher resolutions if details such as mesoscale fronts are to be simulated. On the other hand, it is also necessary to simulate the

evolving synoptic-scale environment as this affects both polar low development and movement. In general, the synoptic-scale flow plays a primary role in steering mesoscale cyclones in a passive manner. However if two or more polar lows are active within close proximity it is possible that they will interact and this also affects their movement. Hence forecasting polar low tracks stretches current numerical modeling resources as it requires both high resolution and large domain sizes.

In an operational context, the simulation of polar lows is still very much in its infancy. At present global operational models are at the limits of resolution necessary to capture polar mesoscale cyclones: often they are subgrid-scale. While regional operational models may well be of sufficient resolution, these tend to be focussed on population centers rather than the polar regions. Over coming years, there is no doubt that advances in computing will lead to higher resolutions for operational forecasting and, if the experience of research numerical-modeling is echoed, this should lead to an ability to routinely simulate mesoscale cyclones in operational numerical weather prediction. A key question then will be: are the operational observing and data assimilation systems good enough to analyse mesoscale cyclones? Many of the remotely-sensed data discussed earlier are now routinely assimilated into operational numerical weather prediction models, but it remains to be seen how accurate routine analyses are in representing polar lows and polar mesoscale cyclones.

Key Words

polar lows; mesoscale cyclones; arctic instability lows; comma clouds; polar mesocyclones; vortices; baroclinic instability; potential vorticity; CISK; WISHE; air-sea heat fluxes; Nordic Seas; convection; hurricanes; extratropical cyclones;

See also

Air-sea interaction: Momentum, heat and vapour fluxes (64);
Baroclinic instability (76);
Cyclones: Extratropical cyclones (128);
Hurricanes (474, 164);
Instability: Conditional/Convective (174);
Instability: Wave-CISK (177);
Mesoscale meteorology: models (217);
Potential Vorticity (320);

Further Reading

Craig, G. C. and S. L. Gray, 1996: CISK or WISHE as the mechanism for tropical cyclone intensification. *J. Atmos. Sci.*, **53,** 3528-3540.

Emanuel, K. A. and R. Rotunno, 1989: Polar lows as arctic hurricanes. *Tellus*, **41A,** 1-17.

Grønas, S. and N. G. Kvamsto, 1995: Numerical simulations of the synoptic conditions and development of arctic outbreak polar lows. *Tellus*, **47A,** 797-814.

Hoskins, B. J., M. E. McIntyre, and A. W. Robertson, 1985: On the use and signficance of isentropic potential vorticity maps. *Quart. J. Roy. Met. Soc.*, **111,** 877-946.

Rasmussen, E., 1979: The polar low as an extratropical CISK disturbance. *Quart. J. Roy. Met. Soc.*, **105,** 531-549.

Rasmussen, E. and J. Turner, 2002: *Polar lows*. Cambridge University Press.

Shapiro, M. A., L. S. Fedor, and T. Hampel, 1987: Research aircraft measurements of a polar low over the Norwegian Sea. *Tellus*, **39a,** 272-306.

Turner, J., T. Lachlan-Cope, and J. Thomas, 1993: A comparison of Arctic and Antarctic mesoscale vortices. *J. Geophys. Res.*, **98,** 13019-13034.

Twitchell, P. F., E. A. Rasmussen, and K. L. Davidson, 1989: *Polar and arctic lows*. A Deepak, 421 pp.

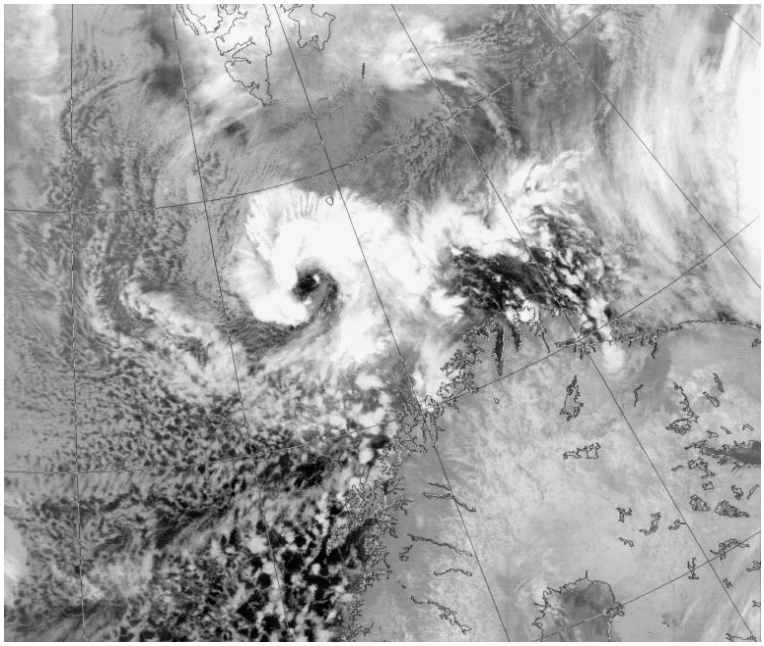

Figure 1 Infra-red satellite image of the Barents Sea area at 02:40 UTC 13 December 1982. Light colours represent cold brightness temperatures. A polar low is well defined by a cloud vortex with a clear central eye.

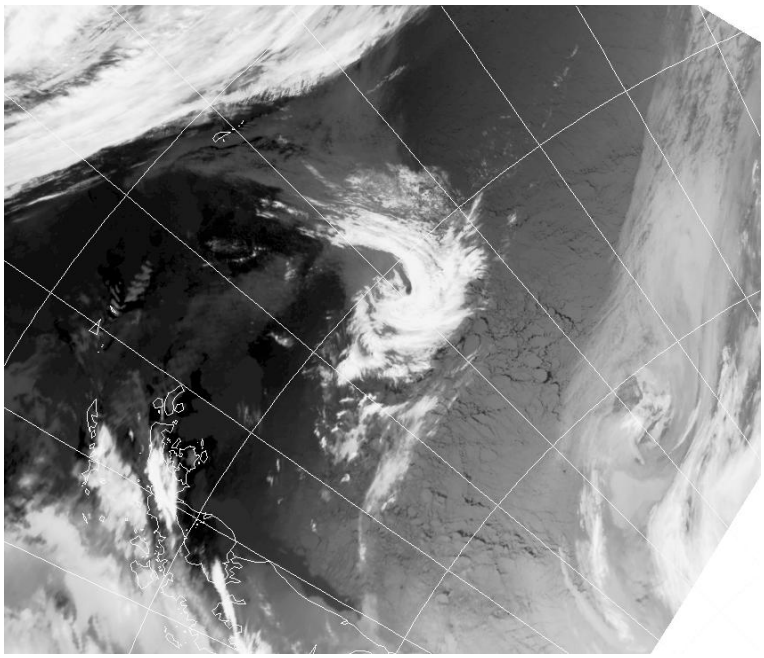

Figure 2 Infra-red satellite image of the sea ice covered Weddell Sea area at 17:30 UTC 6 October 1995. A polar mesoscale cyclone is clearly defined by the comma-shaped cloud vortex.

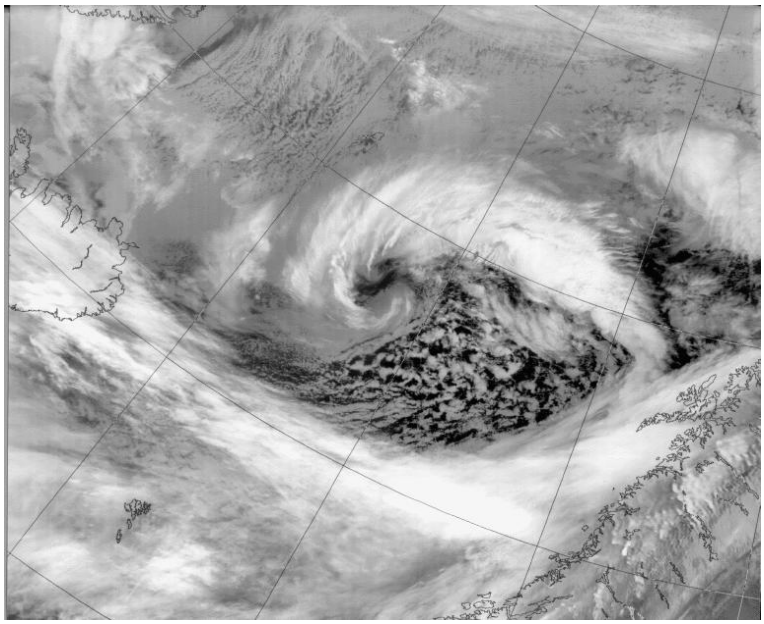

Figure 3 Infra-red satellite image of the Norwegian Sea area at 13:40 UTC 27 February 1984. A polar low with a well-defined clear central eye is visible.

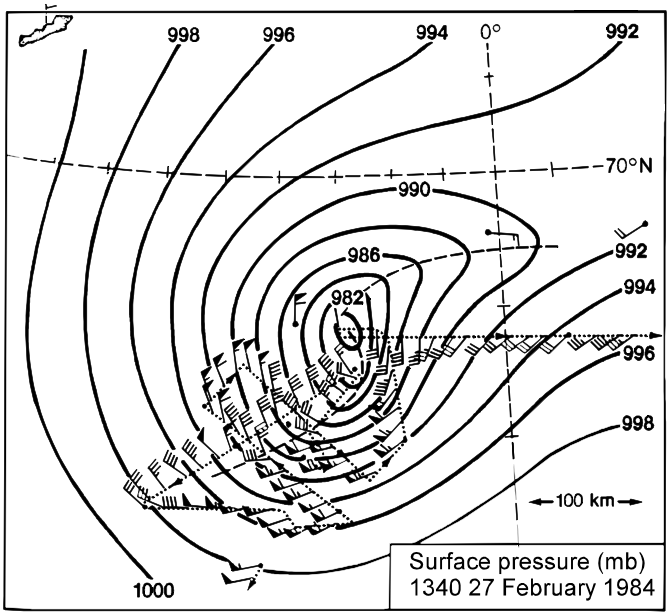

Figure 4 A surface pressure analysis for 13:40 27 February 1984. Overlaid is the track of the instrumented aircraft and the observed flight-level winds. Each full-tick on the wind barbs is 5 m s^{-1}. S-shaped mesoscale fronts curving to the northeast and the southwest are depicted as dashed lines. Adapted from Shapiro et al. (1987) with permission.

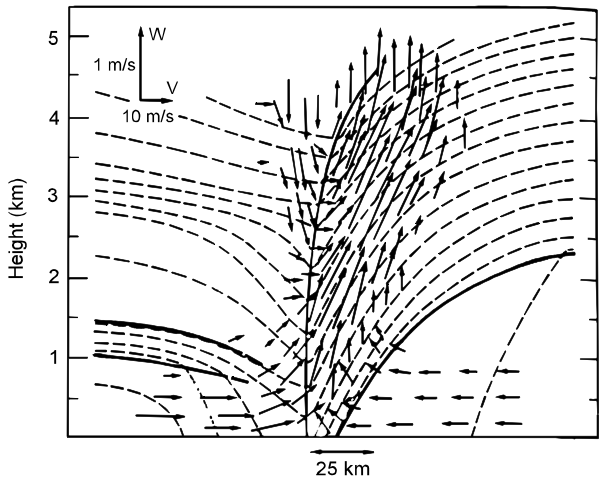

Figure 5 A cross-section through the polar low of 27 February 1984, running approximately north-south at about 4°W. The dashed lines show potential temperature (every 1 K). The solid lines delineate the capping of the near-neutral marine boundary layer and the frontal boundary. The vectors show the storm-relative transverse circulation. Adapted from Shapiro et al. (1987) with permission.

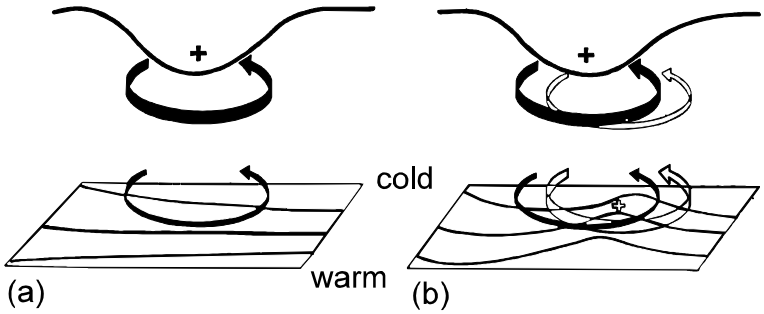

Figure 6 The interaction of an upper-level potential vorticity (PV) anomaly (+ sign) with a low-level baroclinic zone. The cyclonic circulation induced by the upper-level PV anomaly is illustrated through the solid curves. Panel (a) shows the initial state. Panel (b) shows the advection of the low-level potential temperature field into a warm anomaly. At the surface this is equivalent to a positive low-level PV anomaly (open + sign) and thus induces a cyclonic circulation illustrated through the open curves. The interaction is self-reinforcing and leads to rapid cyclogenesis. Adapted from Hoskins et al. (1985) with permission.